

NEES/E-Defense Base-Isolation Tests: Effectiveness of Friction Pendulum and Lead-Rubber Bearings Systems



Tomohiro SASAKI & Eiji SATO

National Research Institute for Earth Science and Disaster Prevention

Keri L. RYAN

University of Nevada, Reno

Taichiro OKAZAKI

Hokkaido University

Stephen A. MAHIN

University of California, Berkeley

Koichi KAJIWARA

National Research Institute for Earth Science and Disaster Prevention

SUMMARY:

This is one of four papers reporting a NEES/E-Defense collaborative program on base-isolated buildings. A full-scale, five-story, two-by-two bay, steel moment-frame building was subjected to a number of bidirectional and bidirectional-plus-vertical ground motions using the E-Defense shake table. The building was tested under three different configurations: 1) base isolated with triple-friction-pendulum bearings (TPB), 2) base isolated with a combination of lead-rubber bearings (LRB) and cross-linear bearings (CLB), and 3) base fixed. This paper introduces the results of shake table experiments on full-scale base-isolated building and shows the effectiveness of recent base-isolation techniques for frequent, near-fault and long duration subduction earthquakes. Based on experimental results, it was found that TPB system provided greater attenuation of floor accelerations for the ground motions with PGA larger than 10 m/s^2 while LRB-CLB system provided greater attenuation of floor accelerations for ground motions with PGA smaller than 5 m/s^2 .

Keywords: seismic design, base-isolation, triple friction pendulum bearing, lead-rubber bearing, steel moment frame building

1. INTRODUCTION

This is one of four papers reporting a collaborative program on base-isolated buildings conducted under the Memorandum of Understanding between the National Research Institute for Earth Science and Disaster Prevention (NIED) of Japan and the National Science Foundation (NSF), George Brown Jr. Network for Earthquake Engineering Simulation (NEES) program of the U.S.

Base isolation is one of the most effective measures to protect building structures and their nonstructural components from earthquake ground motions. Development of modern seismic isolation technique started in the 1960's in New Zealand (Skinner et al., 1993). Various forms of elastomeric bearings such as natural rubber bearings, high damping rubber bearings, and lead-rubber bearings have been commercially implemented since the 1980's. The friction pendulum bearing is a newer base isolation device that was first developed in the late 1980's (Zayas et al., 1987) and whose implementation to buildings started from a seismic retrofit project in 1994. Currently, a wide range of base isolation devices are commercially available and are being implemented in practice. However, wide acceptance of base isolation has not happened yet partly because their cost benefit is not well understood in the structural engineering community.

Consequently, a large-scale, shake-table test program was conducted with a goal of promoting rapid spread of base isolation systems in Japan and the U.S. In this program, a full-scale, five-story, steel

moment-frame building was subjected to a number of bidirectional and bidirectional-plus-vertical ground motions using the world’s largest shake table, E-Defense. The building was tested under three different configurations: 1) base isolated with triple-friction-pendulum bearings (TPB), 2) base isolated with a combination of lead-rubber bearings (LRB) and cross-linear bearings (CLB), and 3) base fixed. This paper compares the response obtained for the three configurations and discusses the effectiveness of recent base-isolation techniques to protect buildings, along with its contents and nonstructural elements, from frequent, near-fault, and long duration subduction earthquakes.

2. SPECIMEN AND EXCITATION

2.1. Steel Moment-Frame Building

Fig. 1 shows the superstructure used in the shake table tests. The superstructure was a five-story, two bay-by-two bay steel moment-frame building that was designed and tested in a previous program by Kasai et al. (2010). While dampers were placed in four of the five stories in the previous program, the dampers were removed from the building for this program. As shown in Fig. 1, X and Y directions were defined as the direction of short and long sides of the slabs and Z direction was defined as the vertical direction. The building was 15.8-m tall and had a floor plan dimension of 10 m by 12 m. The columns used 400-mm deep square hollow sections with thickness ranging between 12 and 22 mm. The girders and beams used wide flange sections with dimension of 400 mm × 200 mm, 300 mm × 150 mm, and 198 mm × 99 mm. The base beams were relatively rigid wide flange beams with dimension of 900 mm × 500 mm. All girder-to-column and column base connections were fully-restrained moment connections. Each girder had short end segments welded to the column in shop, and the remaining middle segment of the girder was spliced in the field by bolting. The girder flanges were widened near the connections to the column to avoid fracture at the critical welds. At the second to fifth floors, composite slabs were formed from 75-mm height corrugated steel decks covered by 80-mm thick normal concrete. The roof slab was a 150 mm thick normal concrete slab with a flat steel deck. The total weight of the building was 486 tons. A 56-ton steel mass was added on the east side and middle of the roof to represent a penthouse and to intentionally introduce eccentricity in mass and weight.

Nonstructural components were installed on the fourth and fifth floors. U.S.-style suspended ceiling grid systems, interior walls, and piping systems were installed using U.S. material and construction techniques. The architectural layout included enclosed rooms to allow for the enactment and portrayal of hospital and office rooms including a variety of furniture and other loose items. In addition, two full story pre-cast concrete cladding panels were set between the fourth and fifth floors to evaluate the effectiveness of current slotted steel connection design to allow story drift. Details of the nonstructural

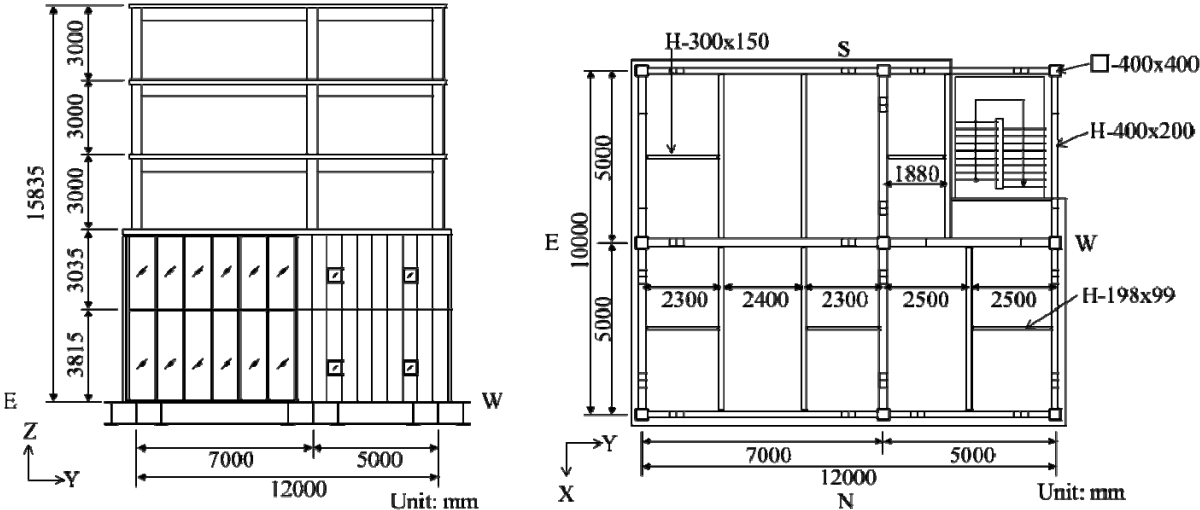


Figure 1. Five-story Steel Moment Frame Building

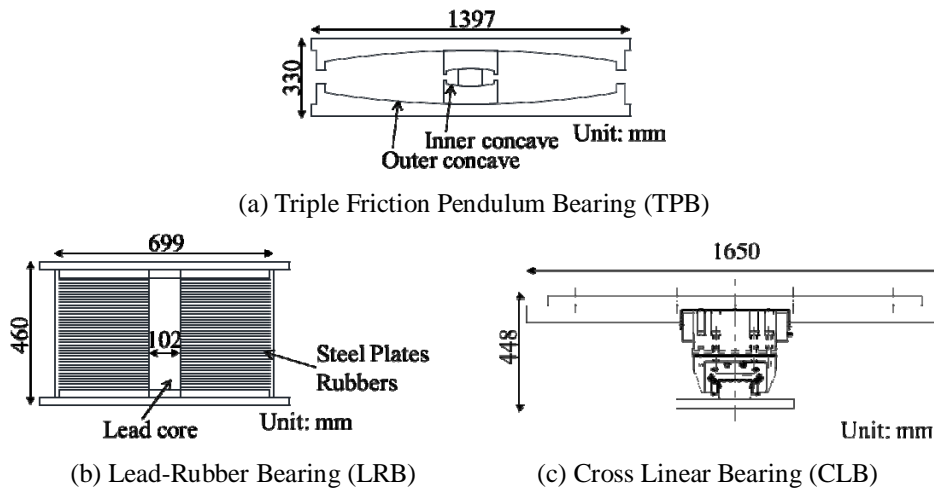


Figure 2. Isolation Devices

components and their behavior are reported in a companion paper by Soroushian et al. (2012).

2.2. Base-Isolation Devices

Two different base isolation systems were devised for the shake table program. The first system placed nine triple friction pendulum bearings (TPB) under each of the nine columns. The second system was a combination of four lead-rubber bearings (LRB) and five cross linear bearings (CLB). Fig. 2 shows isolation devices used in this study. After testing of the two base-isolation systems was completed, the superstructure was directly tied to the shake table and tested under the base-fixed condition.

The TPB system was designed to meet specific performance objectives for U.S. MCE and Japan L3 event. U.S. MCE spectrum was computed from spectral coefficients $S_{MS} = 2.2g$ and $S_{M1} = 1.11g$ at 0.2 and 1.0 seconds, respectively, assuming a Los Angeles location with site class D (ASCE 2010). The Japan L3 spectrum was computed as a 50% increase over an L2 event at the site with the soil type II in Zone A seismicity, which applies to most regions of Japan (AIJ, 2001 and Pan et al., 2005). The design parameters of TPB such as friction coefficients, effective pendulum lengths and displacement capacities of the three independent pendulum mechanisms were selected to achieve the target demands of floor accelerations $< 0.35g$ and story drifts $< 0.5\%$. The TPBs were 1.4 m in diameter, 0.33-m tall, with displacement capacity of 1.13 m. The natural periods were 1.84 and 5.57 seconds, and friction coefficients were 0.02 and 0.08 in the inner and outer pendulum mechanisms, respectively.

The LRB-CLB system placed LRBs under the four edge columns and CLBs under the four corner and one center column, considering the relatively light weight of the steel moment-frame building. The LRB-CLB system was designed to protect a nuclear power plant in beyond-design-basis shaking. In this project, design-basis shaking was determined as ground motions with an annual probability of exceedance of 10^{-5} for a representative eastern U.S. soil site, where the design spectrum was determined from a site specific analysis (Huang et al. 2009). The LRBs were 0.699 m in diameter and 0.46-m tall. Assuming a constant axial force of 1,325 kN per bearing based on the tributary gravity load, these LRBs provide a yield strength coefficient of $V/W = 0.055$ and a post-yield natural period of 2.86 sec. The CLBs were 0.448 m tall and comprised two 1.65-m long rails in two orthogonal directions. Each rail had a displacement limit of ± 0.6 m. The CLBs were rated to provide a low friction coefficient of 0.0019 under a constant vertical compression of 485 kN.

2.3. Instrumentation

More than 650 sensor channels were used to measure the response of the isolation system, the superstructure, and the nonstructural components. For the isolation system, wire potentiometers were used to measure the bidirectional displacements and an assembly of tri-axial load cells was installed under each bearing to measure the forces. For the superstructure, accelerometers were placed on three

corner columns on each floor. Additional accelerometers were placed on the floor slab to measure floor vibration. Laser-type displacement transducers were used to measure the story drift of each story. More than 200 channels were devoted to nonstructural components. Accelerometers and displacement transducers were placed on ceiling, interior walls, piping, and exterior pre-cast walls to measure their dynamic response.

2.4. Excitation Plan

The building was subjected to various ground motions in each of the three configurations. The shake table tests were conducted over six days; three days for the TPB system, two days for the LRB-CLB system, and one day for the fixed-base case. The motions for the TPB system were selected with the objective of subjecting the system to a wide variety of strong ground motions with different characteristics, ranging from intense high frequency content (e.g. JMA Kobe record from the 1995 Kobe earthquake), near fault (e.g. Sylmar record from the 1994 Northridge earthquake), very long period (e.g. ChiChi TCU065 record from the 1999 ChiChi earthquake), to long-duration subduction (e.g. Iwanuma record from the 2011 Tohoku earthquake). The motions for LRB-CLB system were selected primarily with the objective of approaching the displacement limit of the system using synthetic motions representative of potential nuclear sites that had been studied by Huang et al. (2009) (i.e., Vogtle on the U.S. east coast and Diablo Canyon on the west coast). The motions for the fixed-base case were selected with the objective of establishing a base of comparison between isolated and fixed-base buildings. The motions for the fixed-base case were scaled down to maintain the structure response within the linear range. In addition to the primary excitations, white noise and sweep excitations were conducted to enable system identification in the fixed-base configuration.

This paper uses the data obtained from three motions, Westmorland, Iwanuma, and Rinaldi records, to compare the response of the building under the different configurations. All three are recorded motions. Fig. 3 shows the time history of the three target motions, while Fig. 4 shows the response acceleration and displacement spectra. For reference, Fig. 4 indicates the Japan L1, L2, and L3 design spectrum. The Westmorland motion was the obtained at Westmorland from the 1987 Superstition Hills earthquake. For this program the original motion was scaled down to 80% for all three configurations. The Iwanuma motion was obtained at Iwanuma, Miyagi, from the 2011 Tohoku earthquake. The 100% horizontal motion was used for the TPB and LRB-CLB systems and the 70% horizontal motion

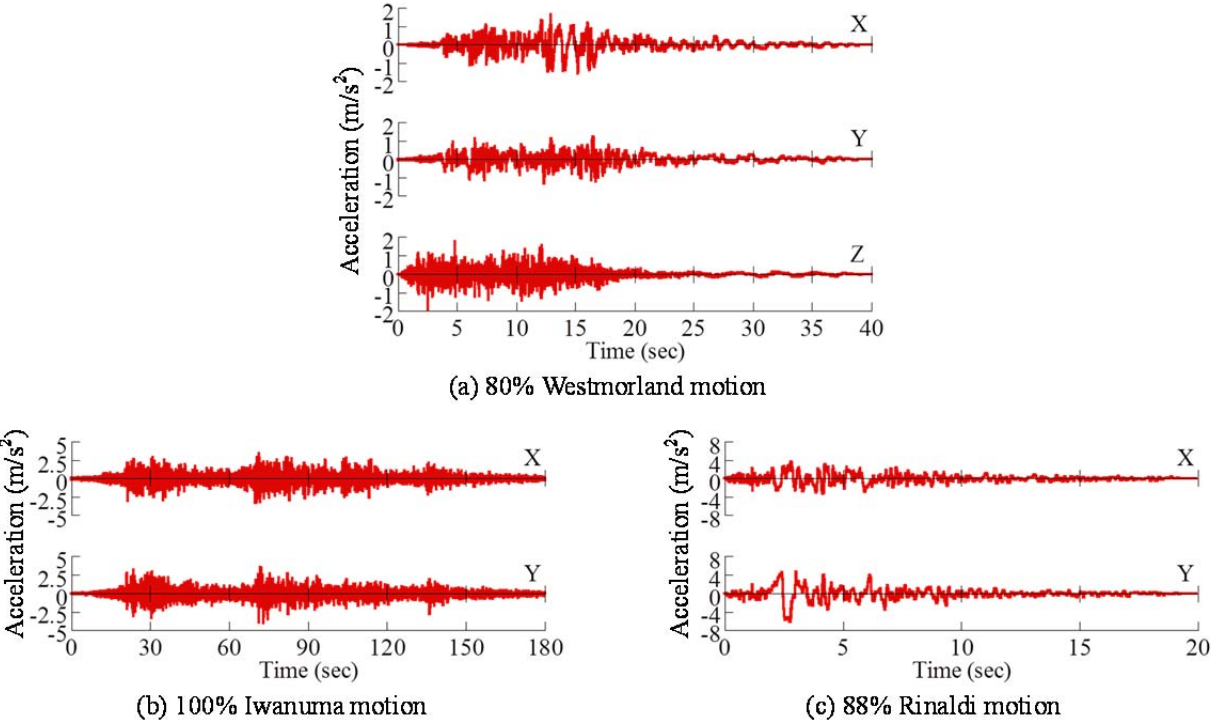
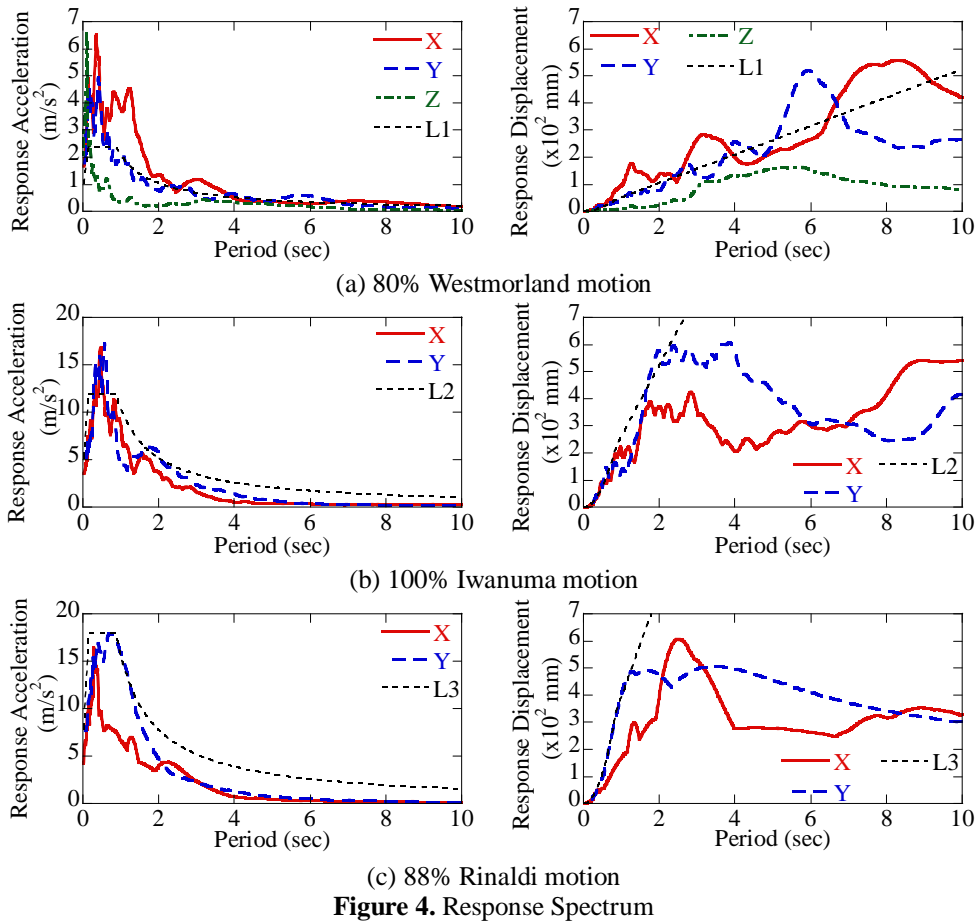


Figure 3. Imposed motions



was used for the fixed-base case. The Rinaldi motion was the obtained at Rinaldi Receiving Station from the 1994 Northridge earthquake. The Rinaldi motion is characterized by extremely strong vertical components. An 88% horizontal-only motion was used for the TPB and LRB-CLB systems, while a 35% horizontal-only motion was used for the fixed-base case. The response to 3D Rinaldi excitation, which was another motion used for all three configurations, is the subject of a companion paper by Ryan et al. (2012) and is not discussed in this paper.

3. SYSTEM IDENTIFICATION OF SUPERSTRUCTURE

Fig. 5 shows the transfer functions determined from the white noise excitation conducted for the fixed-base case prior to the primary excitations. The period and damping ratio corresponding to the fundamental response modes were evaluated by curve fitting theoretical transfer functions to the measured transfer functions using a least square algorithm. It should be noted that, because rocking motion of the table affected the system identification results significantly, Eqs. 19 and 20 in Kasai et al. (2011) were used to eliminate the rocking motion. Table 1 and Fig. 6 summarize the evaluated periods

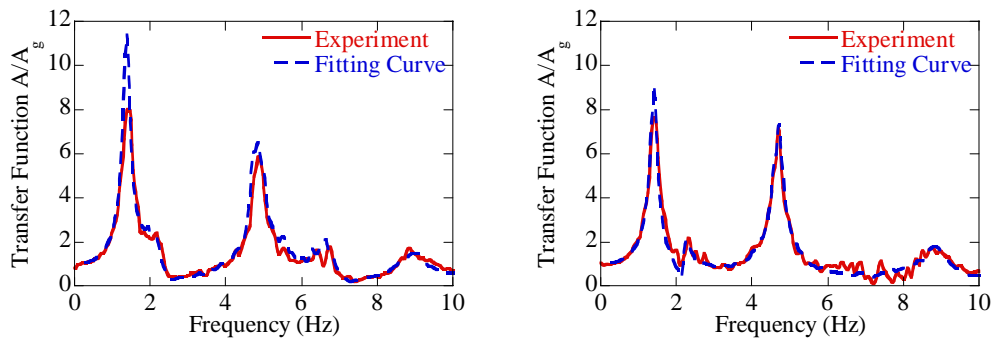
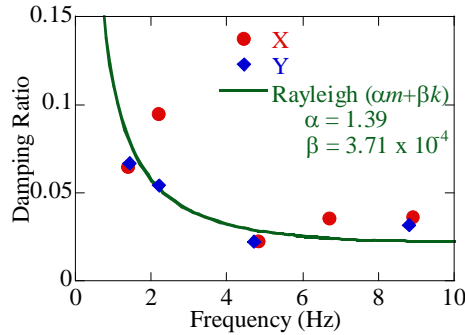


Table 1. Natural Periods and Damping Ratios

(a) X direction			(b) Y direction		
	Period (sec)	Damping Ratio		Period (sec)	Damping Ratio
1st	0.718	0.0643	1st	0.702	0.0668
2nd	0.454	0.0946	2nd	0.452	0.0545
3rd	0.207	0.0223	3rd	0.212	0.0224
4th	0.149	0.0355	4th	0.113	0.0315
5th	0.112	0.0363	5th	0.073	0.0342
6th	0.074	0.0239	6th	0.055	0.0185

**Figure 6.** Damping Ratio

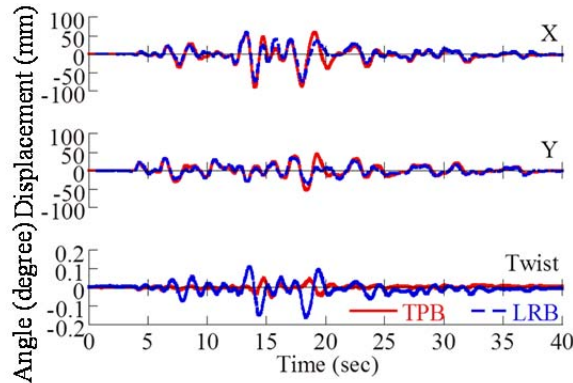
and damping ratios. As indicated in Fig. 6, the damping ratios can be reasonably approximated by Rayleigh damping with coefficients $\alpha = 1.39$ and $\beta = 3.71 \times 10^{-4}$.

4. EXPERIMENTAL RESULTS

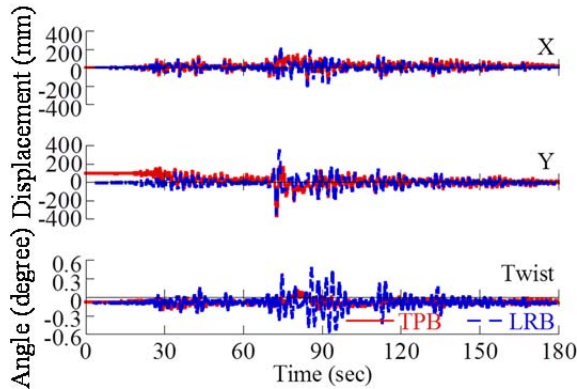
4.1. Isolator Response

Fig. 7 shows the bidirectional displacement and twist angle obtained from the TPB and LRB-CLB systems for each of the three motions. For the 80% Westmorland motion shown in Fig. 7(a), the horizontal displacements in the two systems were surprisingly similar to each other considering the difference in their effective natural periods. For the 100% Iwanuma motion shown in Fig. 7(b), the peak isolator displacements were very similar, reaching 368 mm in the TPB system and 347 mm in the LRB-CLB system. On the other hand, the twist angle was substantially larger in the LRB-CLB system than in the TPB system. For the 88% Rinaldi motion shown in Fig. 7(c), the peak twist angle in the LRB-CLB system was 0.96° , which corresponds to a 201-mm difference in X-displacement between the east and west edges. In the TPB system, twist angle was 0.19° , which corresponds to a mere 4-mm difference in X-displacement between the two edges. Because the horizontal reaction of the TPB is proportional to the vertical force (Zayas et al., 1987), the center of gravity always coincides with the center of reaction in TPB systems.

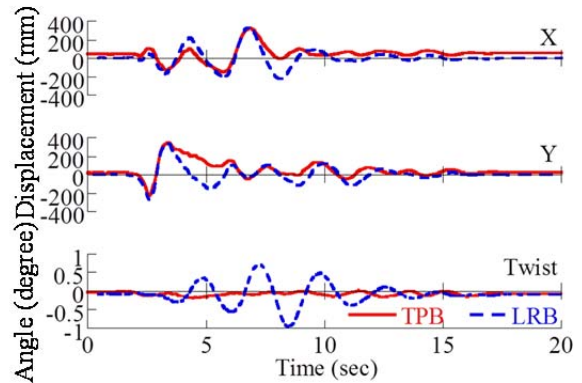
Fig. 8 shows the hysteresis of the isolation layer for each of the three motions, plotting the base shear against isolation layer displacement. For the 80% Westmorland motion shown in Fig. 8(a), the hysteretic loop was very similar between the TPB system and LRB-CLB system. It was observed in the TPB system that, because the response displacement was small such that sliding occurred only along the inner sliding surface and the outer sliding was not activated, the natural period was close to the effective period of the LRB-CLB system. For the 100% horizontal-only Iwanuma motion shown in Fig. 8(b), the peak base shear reached 1,187 kN ($= 0.224W$) in LRB-CLB system and 719 kN ($= 0.135W$) in TPB system. For the Rinaldi motion shown in Fig. 8(c), the TPB system exhibited a very uneven hysteretic loop. As discussed further in a companion paper by Okazaki et al. (2012), the uneven hysteresis was due to substantial uplift in several TPBs.



(a) 80% Westmorland motion

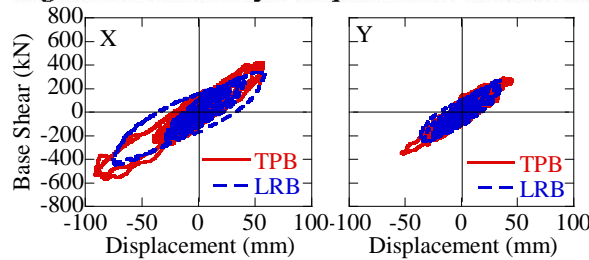


(b) 100% Iwanuma motion

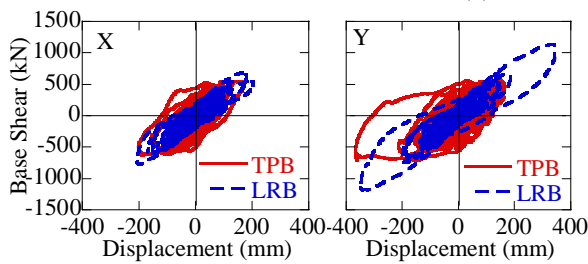


(c) 88% Rinaldi motion

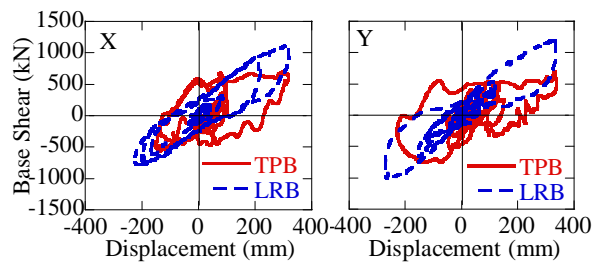
Figure 7. Isolation Layer Displacement and Twist Angle



(a) 80% Westmorland motion



(b) 100% Iwanuma motion



(c) 88% Rinaldi motion

Figure 8. Base Shear vs. Isolation Layer Displacement Hystereses

4.2. Floor Accelerations

Figs. 9 and 10 shows the floor accelerations in the Y direction measured from the 100% Iwanuma and 88% Rinaldi motions. The acceleration histories were taken from the first and fifth floors for the TPB and LRB-CLB systems and from the fifth floor for the fixed-base case. The floor acceleration was substantially smaller in the TPB system than in the fixed-base case. While the same can be said for the LRB-CLB system, this system experienced several impulse accelerations at the first floor. The impulse was caused by slipping of the bolts at the top and bottom connections of the LRBs. Due to experimental constraints, a minimal number of bolts were used for these connections. However, these

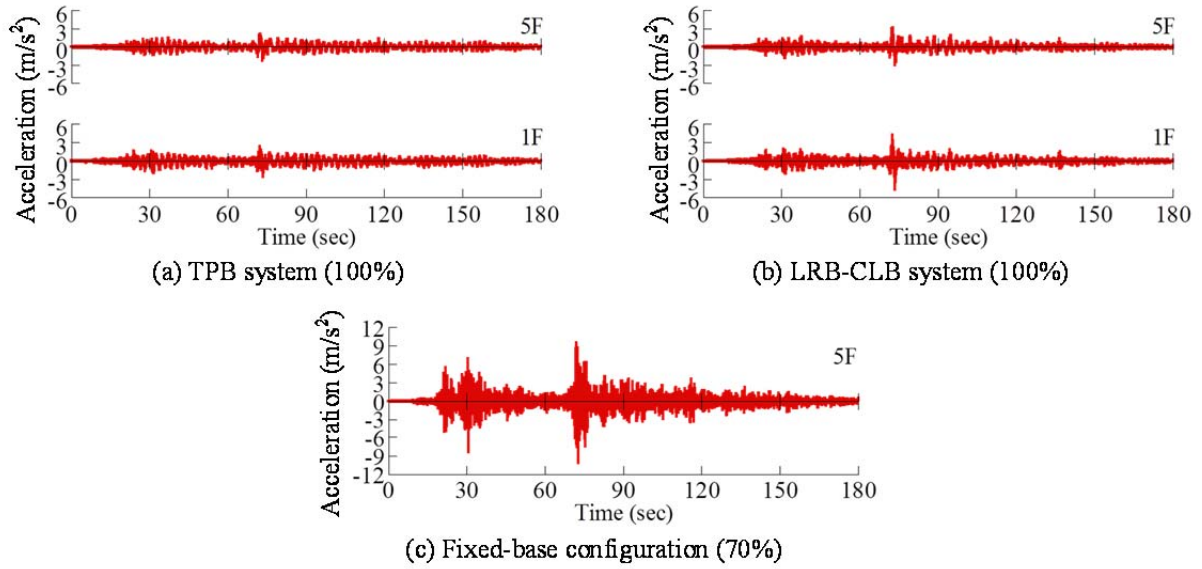


Figure 9. Floor Acceleration in Y direction (Iwanuma motion)

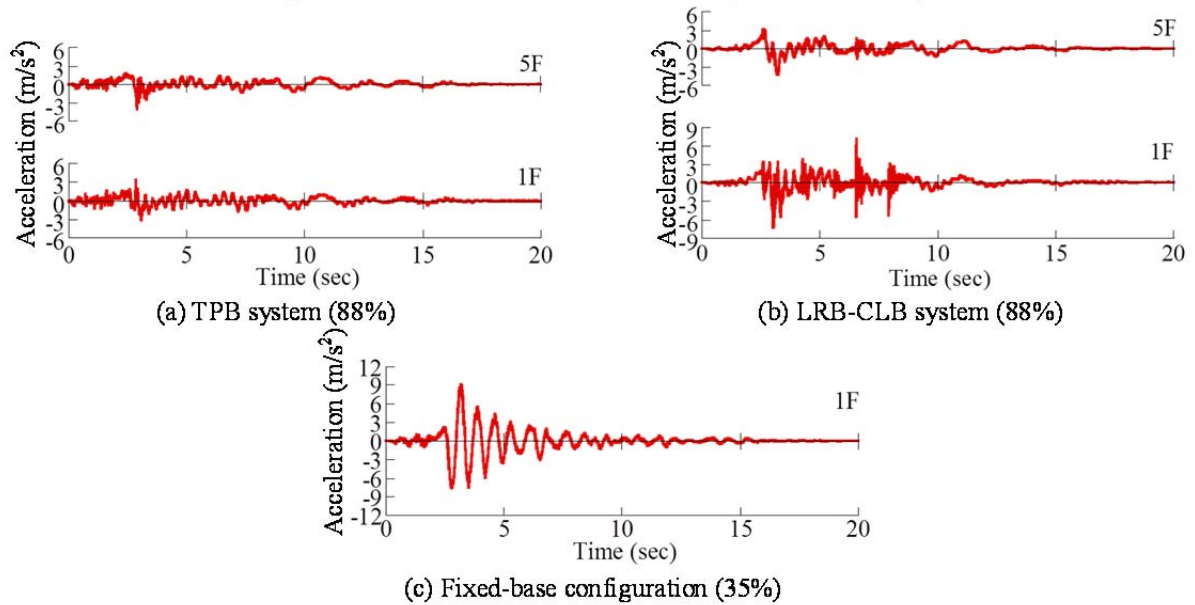
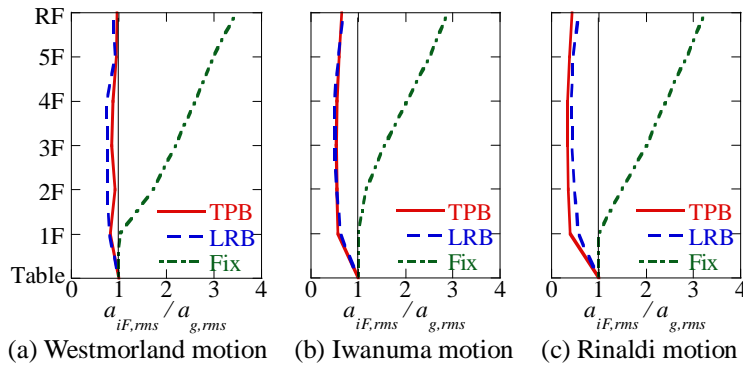


Figure 10. Floor Acceleration in Y direction (Rinaldi motion)

impulses did not cause damage to the superstructure. Because the impulse motion was not transmitted to the upper floors, the impulse did not cause damage to the loose contents or the nonstructural elements. In conclusion, Figs. 9 and 10 suggest that both isolation systems worked effectively and as intended.

Fig. 11 plots the ratio of root-mean-square (RMS) between the floor acceleration $a_{iF,rms}$ and table acceleration $a_{g,rms}$, evaluated for all floors. The fixed-base case experienced response amplification in the form of $a_{iF,rms}/a_{g,rms}$ exceeding unity and increasing with floor height. However, the $a_{F,rms}/a_{g,rms}$ value was below unity in both isolation systems, indicating that both isolation systems worked as intended for frequent (80% Westmorland), long duration subduction (100% Iwanuma), and near fault (88% Rinaldi) ground motions.

The amplification factor $a_{F,rms}/a_{g,rms}$ measured from the 80% Westmorland motion (Fig. 11(a)) was 0.84 to 0.95 for the TPB system and 0.73 to 0.92 for the LRB-CLB system. Interestingly, the factor measured from the 88% Rinaldi motion (Fig. 11(c)) was smaller at 0.33 to 0.44 for the TPB system and 0.42 to 0.56 for the LRB-CLB system. The peak measured table acceleration was 1.49-1.53 m/s² and 11.25-12.03 m/s² for the Westmorland and Rinaldi motion, respectively. Therefore, the



(a) Westmorland motion (b) Iwanuma motion (c) Rinaldi motion
Figure 11. Ratio of RMS between Response Acceleration and Table Acceleration (Y direction)

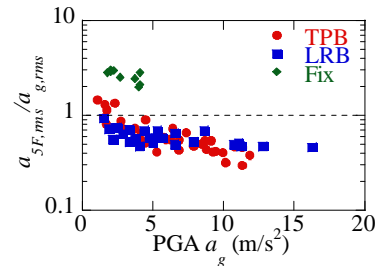


Figure 12. Dependence of Acceleration Amplification Factor by Isolation Devices on Peak Table Acceleration (Fifth floor)

comparison indicates that both isolation systems were more effective for motions with larger PGAs. Also, the TPB system provided greater attenuation of floor acceleration than the LRB-CLB system against motions with larger PGA, during which the TPB system response was dominated by sliding on the outer pendulum surfaces, with an isolation period of 5.57 sec compared to 2.86 seconds for LRB-CLB. However, the LRB-CLB system provided greater attenuation of floor acceleration against motions with smaller PGA, during which the TPB system response was dominated by sliding on the inner sliders, with an isolation period of only 1.84 seconds. These observations are a result of the isolation periods provided by the systems, and not the mechanics of the bearing devices.

Fig. 12 summarizes the relationship between the amplification factor at the fifth floor $a_{5F,rms}/a_{g,rms}$ and PGA computed for all motions imposed to the specimen expect for 3D Rinaldi motion containing strong vertical acceleration. As observed from Fig. 11, the LRB-CLB system tended to be more effective than the TPB system when PGA was smaller than 5 m/s^2 . Recall that the TPBs used for the specimen were designed to respond rigidly until the horizontal force overcomes the friction force between the inner sliding surfaces, $0.02W$. However, when the PGA exceeded 10 m/s^2 , the TPB system tended to be more effective than the LRB-CLB system in reducing the amplification factor.

4.3. Damage to Nonstructural Components

The photographs in Fig. 13 show the damage to nonstructural components observed for the fixed-base case. During the 35% horizontal-only Rinaldi motion, contents moved violently and items fell from shelves. Damage to the ceiling system was limited to minor cracking around the sprinkler heads. During the 70% horizontal-only Iwanuma motion, the ceiling system suffered damage such as falling of panels and bending of the metal members comprising the grid. After testing, the tables and shelves had moved and almost all loose items had dropped to the floor. In contrast, for the TPB and LRB-CLB systems, no damage was observed in the ceiling systems, interior walls, or piping. Movable contents such as chairs with wheels rolled around, but otherwise, no damage was observed in the contents.



(a) 35% Rinaldi motion (b) 70% Iwanuma motion
Figure 13. Damage to Nonstructural Systems in Fixed-base Configuration

5. CONCLUSIONS

A large-scale shake-table test program was conducted under the collaborative research program between E-Defense and NEES with a goal of promoting rapid spread of base-isolation systems in Japan and the U.S. Based on the experimental results, the following conclusions are deduced;

- 1) In both the TPB and LRB-CLB isolation systems, the peak floor accelerations were smaller than those measured in fixed-base case. Both isolation systems successfully mitigated damage in the superstructure from a range of strong ground motions. The amplification factor, which is the ratio of root-mean-square values of the floor acceleration and table acceleration $a_{F,rms}/a_{g,rms}$, measured from the 80% Westmorland motion with PGA of 1.49-1.53 m/s² was 0.84 to 0.95 for the TPB system and 0.73 to 0.92 for the LRB-CLB system. The amplification factor measured from the 88% Rinaldi motion with PGA of 11.25-12.03 m/s² was smaller at 0.33 to 0.44 for the TPB system and 0.42 to 0.56 for the LRB-CLB system. In both systems, the amplification factor decreased with increasing PGA.
- 2) TPB system provided greater attenuation of floor accelerations for the ground motions with PGA larger than 10 m/s² while LRB-CLB system provided greater attenuation of floor accelerations for ground motions with PGA smaller than 5 m/s². These observations are a result of the isolation periods provided by the systems.
- 3) Due to the intentional mass eccentricity, the isolation layer was subjected to substantial torsion. While the two systems were not specifically designed for torsion, twisting motion was more effectively mitigated in the TPB system than in the LRB-CLB system.

ACKNOWLEDGEMENT

Funding for this study was provided by NIED, the National Science Foundation through Grants No. CMMI-1113275 and CMMI-0721399, and U.S. Nuclear Regulatory Commission through Contract NRC-HQ-11-C-04-0067. The isolation devices and design service was donated by Earthquake Protection Systems, Dynamic Isolation Systems, and Aseismic Devices Company. The views reflected in this paper are those of the authors alone and do not necessarily reflect those of the sponsors.

REFERENCES

- American Society of Civil Engineers (2010). Minimum Design Loads for Buildings and Other Structures, *ASCE Standard ASCE/SEI 7-10*, Reston, VA, USA.
- Architectural Institute of Japan (2001). *Recommendation for the Design of Base Isolated Structures* (in Japanese).
- Huang, N. Y., Whittaker, A. S., Kennedy, R. P. and Mayes, R. L. (2009). Assessment of Base-Isolated Nuclear Structures for Design and Beyond-Design Basis Earthquake Shaking, *Tech. Report MCEER-09-0008*, University at Buffalo, USA.
- Kasai, K., Ito, H., Ooki, Y., Hikino, T., Kajiwara, K., Motoyui, S., Ozaki, H. and Ishii, M. (2010). Full scale shake table tests of 5-story steel building with various dampers, *Proc. 7th Intern. Conf. on Urban Earthquake Engin. & 5th Intern. Conf. on Earthquake Engin.*, pp. 11-22, Tokyo Institute of Technology, Tokyo, Japan.
- Kasai, K., Murata, S., Kato, F., Hikino, T. and Ooki, Y. (2011). Evaluation Rule for Vibration Period, Damping, and Mode Vector of Buildings Tested by a Shake Table with Inevitable Rocking Motions, *J. Struct. Constr. Eng.*, AIJ, Vol. 76, No. 670, pp. 2031-2040 (in Japanese).
- Okazaki, T., Sato, E., Ryan, K. L., Sasaki, T., Mahin, S. and Kajiwara, K. (2012). NEES/E-Defense Base Isolation Tests: Performance of Bearings, *Proc. 15th World Conf. on Earthquake Engin.*, Lisbon, Portugal.
- Ryan, K. L., Dao, N. D., Sato, E., Sasaki, T. and Okazaki, T. (2012). NEES/E-Defense Base Isolation Tests: Interaction of Lateral and Vertical Response, *Proc. 15th World Conf. on Earthquake Engin.*, Lisbon, Portugal.
- Skinner, R. I., Robinson, W. H. and McVerry, G. H. (1993). *An Introduction to Seismic Isolation*, John Wiley & Sons Inc., NY, USA.
- Soroushian, S., Ryan, K. L., Maragakis, M., Sasaki, T., Sato, E., Okazaki, T., Tedesco, L., Zaghi, A. E., Mosqueda, G. and Alvarez, D. (2012). NEES/E-Defense Tests: Seismic Performance of Ceiling / Sprinkler Piping Nonstructural Systems in Base Isolated and Fixed Base Building, *Proc. 15th World Conf. on Earthquake Engin.*, Lisbon, Portugal.
- Zayas, V., Low, S. and Mahin, S. (1987). The FPS Earthquake Resisting System, *Technical Report UCB/EERC-87/01*, Earthquake Engineering Research Center, University of California, Berkeley, CA, USA.